Fabrication and magnetic control of bacteria-inspired robotic microswimmers

U. Kei Cheang, Dheeraj Roy, Jun Hee Lee, and Min Jun Kim

Citation: Appl. Phys. Lett. **97**, 213704 (2010); doi: 10.1063/1.3518982
View online: http://dx.doi.org/10.1063/1.3518982
View Table of Contents: http://apl.aip.org/resource/1/APPLAB/v97/i21
Published by the American Institute of Physics.

Fabrication and magnetic control of bacteria-inspired robotic microswimmers

U. Kei Cheang,[1] Dheeraj Roy,[2] Jun Hee Lee,[1,3] and Min Jun Kim[1,2,a)]
[1]*Department of Mechanical Engineering and Mechanics, Drexel University, Philadelphia, Pennsylvania 19104, USA*
[2]*School of Biomedical Engineering, Science and Health Systems, Drexel University, Philadelphia, Pennsylvania 19104, USA*
[3]*Nano Convergence and Manufacturing Systems Research Division, Korea Institute of Machinery and Materials, Daejeon 305-343, Republic of Korea*

(Received 15 July 2010; accepted 2 November 2010; published online 23 November 2010)

A biomimetic, microscale system using the mechanics of swimming bacteria has been fabricated and controlled in a low Reynolds number fluidic environment. The microswimmer consists of a polystyrene microbead conjugated to a magnetic nanoparticle via a flagellar filament using avidin-biotin linkages. The flagellar filaments were isolated from the bacterium, *Salmonella typhimurium*. Propulsion energy was supplied by an external rotating magnetic field designed in an approximate Helmholtz configuration. Further, the finite element analysis software, COMSOL MULTIPHYSICS, was used to develop a simulation of the robotic devices within the magnetic controller. The robotic microswimmers exhibited flagellar propulsion in two-dimensional magnetic fields, which demonstrate controllability of the biomimetically designed devices for future biomedical applications. © *2010 American Institute of Physics*. [doi:10.1063/1.3518982]

Recently, the need for controllable micro- to nanoscale devices has increased, which has resulted in several research groups focusing on the development of swimming robots (microswimmers).[1–6] In order to develop microswimmer-based methodologies, these devices must be capable of swimming in low Reynolds number fluidic environments. A majority of currently available macroscale propulsion strategies are unsuitable for functioning in such environments.[7] Berg and Anderson[8] discovered that bacteria swim in fluid environments by rotating their thin helical flagella. Flagellar motors are most suited for low Reynolds number swimming due to their structure and function.[9] Inspired by the bacterial flagella, microswimmers controlled by an external magnetic field have been reported.[1–3] External magnetic fields employed as a wireless energy transfer technique is one way to control microscale robots. Some research groups have tried to use living bacteria to move microscale objects; however, they applied chemicals for the stimulation and control processes, which make such devices unsatisfactory for biological applications.[4] Other groups have developed micromachined devices to achieve controllability in a variety of fluidic environments.[5,6] The drawback of these devices lies in their size being in the millimeter scale. We report the fabrication and control of microswimmers for submillimeter scale applications using flagellar filaments isolated from *Salmonella typhimurium*.

A microswimmer exhibits a dumbbell-like structure composed of a larger polystyrene (PS) bead and a smaller MNP connected via a flagellar filament. The PS bead may be representative of a bead functionalized with drug, while the MNP bead represents the source of microswimmer control in a magnetic environment. The fabrication of microswimmers was carried out using an avidin-biotin link technique. Avidin is a tetrameric protein found in egg white and contains four identical subunits that are capable of binding a biotin group or vitamin B7 in the strongest naturally found noncovalent bond.[10]

The fabrication procedure is divided into three steps: the production of biotinylated flagella, avidin functionalization of beads (PS and MNP), and creation of the microswimmers. For step one, the flagellar filaments are purified from *Salmonella typhimurium* using an ultracentrifugation technique. Briefly, flagellar filaments are mechanically sheared off the bacterial cell bodies. Ultracentrifugation at 35 000 rpm is used to separate the flagella protein from the sheared solution. The purified flagella are depolymerized into monomer subunits and repolymerized to create long flagellar filaments (5–8 μm), which are needed for microswimmer fabrication. A protocol was developed to convert polymerized flagellar filaments into biotinylated flagella. The polymerized flagella were biotinylated at the amino groups of the entire surface of the filament using 25 mg/ml *N*-hydroxysuccinimide-biotin. After biotinylation, the filaments were depolymerized into biotinylated monomers at 65 °C. These biotinylated monomers were utilized in a flagella repolymerization reaction yielding flagellar filaments that had biotin groups at both ends of the filament.

The second step of the fabrication procedure involved avidin functionalization of PS beads and MNPs. For the polystyrene beads, we selected 3 μm with regard to the size of the beads and amino-functionalization for the surface modification, while the magnetic particles are required for propulsion and control within the magnetic controller, and so a size distribution of 150–300 nm was utilized. The avidin functionalization procedure was carried out using 1 mg/ml purified avidin protein dissolved in distilled water, and subsequent incubation of both PS beads and MNPs, for 2 h at room temperature. The avidin protein physically adsorbs onto the surface of the beads due to electrostatic charges. Finally, with the preparation of biotinylated flagella and avidin-functionalized MNPs, the two were combined in a reaction mix to obtain one-bead microswimmers shown in

a)Electronic mail: mkim@coe.drexel.edu.

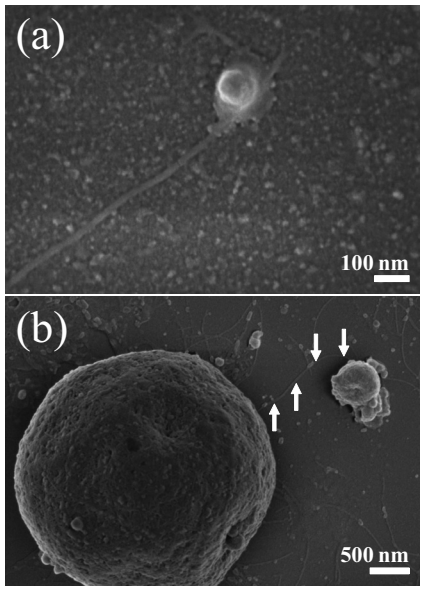

FIG. 1. Scanning electron micrographs of bacteria-inspired robotic microswimmers. (a) 150 nm avidin-functionalized magnetic particle attached to a biotinylated flagellar filament. (b) 3 μm polystyrene bead linked to a 150 nm magnetic particle via a flagellar filament depicting dumbbell or double-bead microswimmers. The flagellar filament linking the two beads is indicated by the arrows.

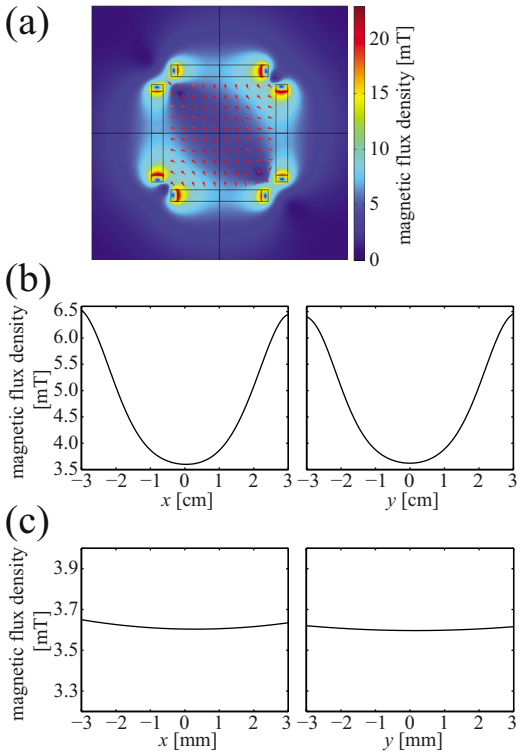

FIG. 2. (Color online) Computational simulation of the electromagnetic controller. (a) Flux and direction of the magnetic field produced by 2 coil pairs. (b) Variations of magnetic field strength in the x (left) and y (right) axes. (c) Variations of field strength along the x (left) and y (right) axes in a 5 mm radius from the center showing a negligible gradient.

Fig. 1(a). The image was taken using a scanning electron microscope (SEM) and it depicts a biotinylated flagellar filament bound at one end to the avidin-functionalized surface of a 150 nm MNP. After observing linkage of avidin-functionalized MNPs to flagellar filaments biotinylated at one end, these one-bead microswimmers were combined with avidin-functionalized PS beads. The resulting sample was imaged using the SEM and double-bead or dumbbell structured microswimmers were visualized, as shown in Fig. 1(b). Figure 1 provides concrete evidence to validate the microswimmer fabrication protocol.

Experimentally, the microswimmers are immersed in distilled water (viscosity of 1 mPa/s) (Ref. 3) within a polydimethylsiloxane (PDMS) chamber with dimensions of 3 mm(length) $\times$ 3 mm(width) $\times$ 2 mm(height). The PDMS chamber served two purposes: minimize fluid flow within the sample and as a result decrease the sinking rate of microswimmers. For microswimmer motion experiments, the sample chamber was placed within a magnetic controller.

The magnetic control system utilizes an approximate Helmholtz setup to generate a uniform magnetic field via two pairs of electromagnetic coils. A LABVIEW algorithm was developed for the control interface, which allowed user input of the magnetic field strength (millitesla), rotational direction of the magnetic bead (clockwise/counterclockwise), and rotational frequency (hertz) of the field. The ac current through the electromagnetic coil pairs generate a rotating magnetic field for microswimmer propulsion. The approximate Helmholtz configuration was created to satisfy the constraint imposed by the physical size of the available microscope stage.

A computational model was developed for predicting the magnetic field generated in the approximate Helmholtz controller as well as its effects on a ferromagnetic particle, assuming a static environment. The magnetic controller can create a rotating magnetic field with near constant strength at the center. Particles located in the central area of the field experience magnetization and align in the direction of the magnetic field. The model simulated a rotating magnetic field using two pairs of coils with a magnetic field composed of x (B_x) and y (B_y) components. The resultant strength (B) can be expressed as

$$B = \sqrt{B_x^2 + B_y^2}.$$

The strength and direction of the magnetic field was determined by the current flowing through the coils. The simulation of the electromagnetic controller consists of coil pairs that are represented by rings with rectangular cross sections. The model generates a magnetic field that has characteristics similar to that of a Helmholtz coil. Figure 2(a) illustrates a surface plot of the magnetic flux density. From the magnetic field computed around a ferromagnetic particle, it was confirmed that the particle is magnetized and develops a magnetic dipole. The applied current is 5 V (2.5 A), which produces a magnetic flux of 3.25 mT at the center of the controller. This value is comparable to the experimental value of 1.81 mT. The area within a 3 mm radius from the center of the field is shown to have a negligible magnetic flux variation ($<2\%$); therefore, it can be assumed that the magnetic field is constant in the sample region. Figures 2(b) and 2(c) plot the variations in magnetic field along the x and y directions, respectively.

The flagella act as helical propellers that convert rotational motion of the MNPs to linear motion of the microswimmers. We have recorded 10 s videos of microswimmer motion using an inverted phase microscope and a vision system (QCAPTURE PRO software). Propulsion experiments were performed using x and z axes magnetic coils to observe microswimmer motion along the y axis in addition to a frequency of 100 Hz, which is comparable to the rotational rate

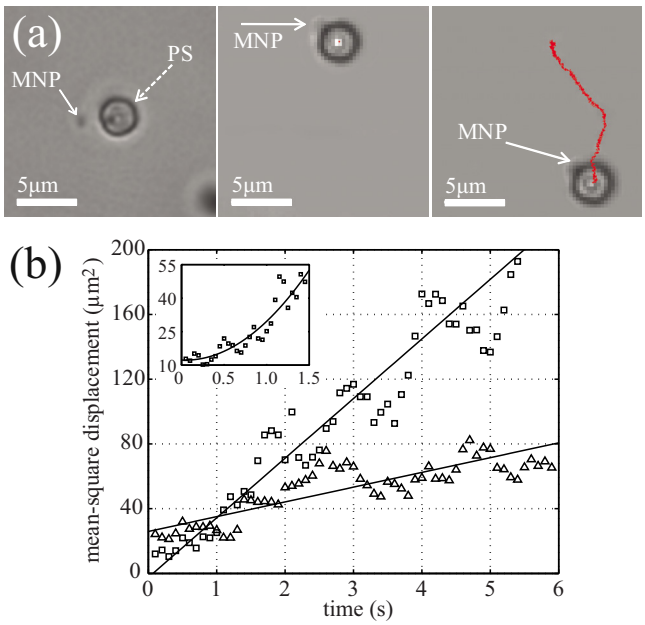

FIG. 3. (Color online) Microswimmer propulsion and mean-square displacement. (a) Visualization of the dumbbell-like microswimmer under 100× objective (left) and path traced by the 3 μm polystyrene bead of a microswimmer over a 10 s interval (middle and right). (b) Mean-square displacement as a function of time, for microswimmer propulsion (open squares) and the no-field condition (open triangles). Linear curve fits of the sample and control groups show an increased diffusion coefficient for the microswimmers (D_{MS}) over the control value (D_{NF}). A curvature exists in the correlation between MSD and $t<1$ s exemplifying the ballistic regime (expanded scale).

of bacterial flagella.[11] In addition, the z axis coils were at a 90° lag relative to the x axis coils in order to orient the microswimmers along the x axis and then create counterclockwise rotation in the z direction. Counterclockwise rotation of flagella is employed by *Escherichia coli* to propel forward in different fluid environments.[9] An output voltage of 10 V (4.5 A) was applied to the working region of the magnetic controller corresponding to a 2.2 mT field strength that is sufficient for microscale propulsion based on published reports of a necessary 2.0 mT (Ref. 3). The video files were imported into MATLAB for tracking analysis based on the centroid of the 3 μm PS bead.

Figure 3(a) shows the path traced by a microswimmer. This image confirmed fabrication of the double-bead microswimmers as well as the orientation of the along the y axis (vertical) within the two-dimensional magnetic field. Further, the microswimmer propulsion follows a vertical directionality that serves as evidence for controlled motion along the y axis. To analyze the magnetic propulsion of the microswimmers, we must account for thermal fluctuation that exists in the micron scale as well as flagellar propulsion.[12] To do so, we calculated the mean square displacement (MSD), which is a measure of the average distance a particle travels in a fluid environment.

$$\mathrm{MSD} = \langle r^2(t) \rangle = \left\langle \frac{1}{N} \sum_{t=0}^{N} [r_1(t) - r_1(0)]^2 \right\rangle,$$

where N is the number of particles, $r_i(t) - r_i(0)$ is the vector distance traveled by a particle over the time interval, and t corresponds to time. Figure 3(b) shows the representative MSD plots. We initially introduced the microswimmers sample into the magnetic controller and recorded a 10 s no-field condition to serve as control, and then applied a 10 V output to capture a 10 s propulsion video. The slope of MSD represents the diffusion coefficient (D). Based on the correlation at small time scale ($t<1$ s), the microswimmer exhibited ballistic motion. At $t>1$ s, the ballistic driven motion transit into a translational diffusive motion.[11,12] The linear regression on a long time scale illustrated the microswimmer propulsion (D_{MS}) with a greater positive slope as compared to the no-field (D_{NF}). From these MSD plots, the two-dimensional D was determined using

$$D = \frac{1}{4} \lim_{t \to \infty} \frac{d}{dt} (\mathrm{MSD}).$$

The D_{MS} and D_{NF} values were 24.19 and 4.38 $\mu m^2/s$, respectively. From the ratio of these coefficients, the microswimmer propulsion results in active diffusion that is approximately six times greater than Brownian (passive) diffusion. With respect to velocity of the microswimmers, an average of 4.1 μm/s was observed. Furthermore, the theoretical diffusion coefficient for a 3 μm sphere in water may be estimated using the Stokes–Einstein equation to compare the diffusion of single PS beads with the diffusion of microswimmers. The theoretical diffusion coefficient is 1.63×10^{-1} $\mu m^2/s$ that is two orders of magnitude smaller than D_{MS} and one order of magnitude smaller than D_{NF}. The theoretical diffusion is smaller than D_{NF} due to the fact that D_{NF} was influenced by PS bead to MNP hydrodynamic interaction,[13] flagellar hydrodynamics, and flow instability, where as the theoretical diffusion accounted only for single PS beads.

In this paper, we demonstrate a controllable, biomimetic device that propels along the direction of interest using flagellar filaments. These robotic microswimming devices can be used in micro- and nanoscale biomedical applications, such as controlled drug delivery with flagellar propulsion, which require three-dimensional controllability in a fluidic environment.

We acknowledge Dal Hyung Kim and Anmiv Prabhu for assistance with particle tracking and support for SEM, respectively. We thank Dr. Boris Polyak for providing the MNPs. The first and second author contributed equally to this work. This work was funded by NSF CBET: Fluid Dynamics Grant No. 0828167.

[1] R. Dreyfus, J. Baudry, M. L. Roper, M. Fermigier, H. A. Stone, and J. Bibette, Nature (London) **437**, 862 (2005).
[2] B. Behkam and M. Sitti, *50 Years of Artificial Intelligence* (Springer, Berlin, Heidelberg, 2007), Vol. 4850, pp. 154–163.
[3] L. Zhang, J. J. Abbott, L. Dong, B. E. Kratochvil, D. Bell, and B. J. Nelson, Appl. Phys. Lett. **94**, 064107 (2009).
[4] B. Behkam and M. Sitti, Appl. Phys. Lett. **90**, 023902 (2007).
[5] K. Ishiyama, K. I. Arai, M. Sendoh, and A. Yamazaki, 2000 International Symposium on Micromechatronics and Human Science, 2000, pp. 65–69.
[6] K. B. Yesin, P. Exner, K. Vollmers, and B. J. Nelson, Medical Image Computing and Computer-Assisted Intervention **3749**, 819 (2005).
[7] E. M. Purcell, Am. J. Phys. **45**, 3 (1977).
[8] H. C. Berg and R. A. Anderson, Nature (London) **245**, 380 (1973).
[9] H. C. Berg, Annu. Rev. Biochem. **72**, 19 (2003).
[10] E. P. Diamandis and T. K. Christopoulos, Clin. Chem. **37**, 625 (1991).
[11] N. Darnton, L. Turner, K. Breuer, and H. C. Berg, Biophys. J. **86**, 1863 (2004).
[12] V. Lobaskin, D. Lobaskin, and I. M. Kulić, Eur. Phys. J. Spec. Top. **157**, 149 (2008).
[13] J. Bammert, S. Schreiber, and W. Zimmermann, Phys. Rev. E **77**, 042102 (2008).